Non-Binary PRN-Chirp Modulation: A GNSS Fast Acquisition Signal Waveform

Article *in* IEEE Communications Letters · June 2022

DOI: 10.1109/LCOMM.2022.3185319

3 authors:

Lorenzo Ortega Espluga
Institut Polytechnique des Sciences Avancées
43 PUBLICATIONS **127** CITATIONS
SEE PROFILE

Jordi Vilà-Valls
Institut Supérieur de l'Aéronautique et de l'Espace (ISAE)
129 PUBLICATIONS **815** CITATIONS
SEE PROFILE

E. Chaumette
Institut Supérieur de l'Aéronautique et de l'Espace (ISAE)
174 PUBLICATIONS **1,039** CITATIONS
SEE PROFILE

Non-Binary PRN-Chirp Modulation: A GNSS Fast Acquisition Signal Waveform

Lorenzo Ortega, Jordi Vilà-Valls, *Senior Member, IEEE*, Eric Chaumette, *Member, IEEE*

***Abstract*—In this article, we propose a new non-binary modulation which allows both Global Navigation Satellite Systems (GNSS) synchronization and the demodulation of non-binary symbols, without the need of a pilot signal, with the aim to provide a fast first position, velocity and time fix. The waveform is constructed as the product of i) a pseudo-random noise sequence with good auto-correlation and cross-correlation properties, and ii) a chirp spread spectrum family, which allows to demodulate non-binary symbols even if the signal phase is unknown. In order to demodulate the data, a bank of non-coherent matched filters is proposed. Because of the particular modulation structure, the receiver is capable to demodulate the navigation message faster while allowing the basic GNSS signal processing functionalities. Illustrative results are provided to support the discussion.**

***Index Terms*—Non-binary modulations, CSS, non-coherent demodulation, Cramér-Rao bound, delay/Doppler MLE.**

I. Introduction

DESIGNING new Global Navigation Satellite Systems (GNSS) signals is always a trade-off between different figures of merit, such as robustness to multipath, precision, or signal compatibility. Recent works addressed the design of fast acquisition signals [1], [2]. Indeed, a big challenges of the new GNSS generation is to provide a fast position, velocity and time (PVT) [3] solution, independently of the receiver conditions. At the so-called *cold state*, no navigation data is available at the receiver and the navigation message must be demodulated, which may take some tens of seconds, being the main time contribution to achieve a PVT solution.

Some recent contributions have proposed different options to reduce the time needed to decode the navigation message (referred to as "time to data" (TTD)). Three main ideas have gained popularity: 1) broadcast a truncated navigation message [4], that is, to reduce the amount of bits used to describe the navigation data. But the PVT precision drastically decreases as a function of the number of removed bits; 2) increasing the symbol rate [5]. Undoubtedly, this can reduce the TTD but only when the channel conditions are favorable. Notice that increasing the symbol rate degrades the symbol demodulation capabilities under harsh scenarios, leading to a trade-off between reducing the TTD in favourable conditions and reducing the symbol demodulation performances (and therefore increasing the TTD) over unfavourable conditions; and 3) navigation message design with redundant bits to protect the information (i.e., the bits used by the channel decoder) [6]. Modern GNSS signals include error correcting schemes in the navigation message in order to identify and correct possible transmission errors. If those error correcting schemes are well-designed (with the maximum distance separable property, e.g., Reed-Solomon [5], LDMDS [2] or root LDPC codes), the receiver may be able to decode the navigation data even if the entire navigation message has not been received. This implies to reduce the TTD without increasing the receiver complexity.

In contrast to the previous alternatives that may have several limitations, we propose the use of non-binary modulations, which have not yet been explored as fast GNSS acquisition signals. Within the GNSS community two non-binary modulations are considered to increase the data rate, namely the Code Shift Keying (CSK) [7], [8] and the Chirp Spread Spectrum (CSS) [9] modulations, but these signals need a synchronization pilot signal to guide the demodulation.

In this work, a new non-binary modulation is proposed, which is constructed as the product of two different modulations: 1) the first one aims to detect the satellite and synchronize with it. A pseudo-random noise (PRN) sequence modulated with generic binary coded symbols (BCS) [10] waveform is proposed due to its good auto-correlation and cross-correlation properties; and 2) the second modulation aims to demodulate the non-binary symbols. To obtain orthogonal non-binary symbol waveforms a family subset of CSS waveforms is considered. The combination of these two modulations leads to a set of waveforms that:

- allows a multi-user communication (thanks to the PRN family), that is, to detect a satellite and estimate its delay and Doppler (synchronization). In contrast to the CSK modulation, there is no need of a pilot signal to demodulate the data (i.e., joint synchronization/demodulation),
- allows non-coherent demodulation (thanks to the family of non-binary orthogonal chirps), where the phase knowledge is not required. Because of the non-binary symbols, the navigation message reception time is reduced.

It is worth pointing out that similar modulations have been proposed in the area of multi-user communications (e.g., refer to [11] and references therein), however those were either binary modulations or required a pilot to be synchronized.

II. Generic Signal Model

Consider the line-of-sight (LOS) transmission of a band-limited signal $s(t)$ (bandwidth B) over a carrier with frequency f_c (wavelength $\lambda_c = c/f_c$), from a transmitter T at position $\mathbf{p}_T(t) = \mathbf{p}_T + \mathbf{v}_T t$ to a receiver R at position $\mathbf{p}_R(t) = \mathbf{p}_R + \mathbf{v}_R t$. The radial displacement between transmitter and receiver is

L. Ortega is with IPSA, Toulouse, France, e-mail: lorenzo.ortega@ipsa.fr; J. Vilà-Valls and E. Chaumette are with ISAE-SUPAERO, University of Toulouse, Toulouse, France, e-mail: {name.surname}@isae-supaero.fr; This research was partially supported by TéSA and the DGA/AID projects (2019.65.0068.00.470.75.01, 2021.65.0070.00.470.75.01).

proportional to the T-to-R signal delay, which is affected by the relative motion between both transmitter and receiver (i.e., Doppler effect). The distance travelled by the signal is

$$\|\mathbf{p}_T\left(t-\tau_0\left(t\right)\right)-\mathbf{p}_R\left(t\right)\| = c\tau_0\left(t\right) \simeq d+vt, \tag{1}$$

with $\tau_0\left(t\right) \simeq \tau + bt, \tau = \frac{d}{c}$ and $b = \frac{v}{c}$, where d is the T-to-R relative radial distance, v the T-to-R relative radial velocity, b a delay drift related to the Doppler effect, c is the speed of light and the unknown parameters to be estimated $\boldsymbol{\eta}^T = [\tau, b]$. Under the narrowband hypothesis [12], [13], i.e., $B \ll f_c$, the Doppler effect on the band-limited baseband signal may be considered negligible: $s((1-b)\left(t-\tau\right)) \simeq s\left(t-\tau\right)$. For an ideal transmitter, propagation channel and receiver, the signal at the output of the receiver's Hilbert filter (I/Q demodulation, bandwidth equal to the sampling frequency F_s) is

$$x\left(t\right) = \beta e^{-j2\pi f_c\left(b\left(t-\tau\right)\right)} s\left(t-\tau\right) + n\left(t\right), \tag{2}$$

with $f \in \left[-\frac{F_s}{2}, \frac{F_s}{2}\right]$, $\frac{F_s}{2} \geq \frac{B}{2}$, $\beta = \beta_A e^{-j2\pi f_c \tau}$, β_A an amplitude factor that depends on the signal power, polarisation vectors, and antenna gains [14], and $n(t)$ a complex white circular Gaussian noise within this bandwidth with unknown variance σ_n^2. The discrete vector signal model is build from $N = N_1 + N_2 + 1$ samples at $T_s = 1/F_s$,

$$\begin{aligned}
&\mathbf{x} = \beta\mathbf{a}(\boldsymbol{\eta}) + \mathbf{n} = \rho e^{j\varphi}\mathbf{a}(\boldsymbol{\eta}) + \mathbf{n}, \\
&\mathbf{x} = \left(\ldots, x\left(kT_s\right), \ldots\right)^\top, \mathbf{n} = \left(\ldots, n\left(kT_s\right), \ldots\right)^\top, \\
&\mathbf{s} = \left(\ldots, s\left(kT_s\right), \ldots\right)^\top, \\
&\mathbf{a}(\boldsymbol{\eta}) = \left(\ldots, s(kT_s-\tau)e^{-j2\pi f_c\left(b\left(kT_s-\tau\right)\right)}, \ldots\right)^\top,
\end{aligned} \tag{3}$$

with $N_1 \leq k \leq N_2$ and $\mathbf{n} \sim \mathcal{CN}\left(\mathbf{0}, \sigma_n^2\mathbf{I}_N\right)$. The unknown deterministic parameters are $\boldsymbol{\epsilon} = \left(\sigma_n^2, \rho, \varphi, \tau, b\right)^\top$, with $\beta = \rho e^{j\varphi}$ ($\rho \in \mathbb{R}^+$, $0 \leq \varphi \leq 2\pi$). Vector $\mathbf{s}$ defines the samples of the baseband transmitted waveform. Notice that each GNSS satellite sequentially broadcasts a known and unique PRN sequence, which is modulated by a binary navigation message.

III. Non-Binary PRN-Chirp Modulation Definition

Let's first consider the well-known linear frequency modulation (LFM) chirp signal classically defined as,

$$\Phi(t) = \Pi_T(t) \times e^{j\pi\alpha t^2},\ \Pi_T(t) = \begin{cases} 1 & 0 \leq t < T \\ 0 & \text{otherwise} \end{cases} \tag{4}$$

with α the chirp rate and $T = NT_s$ the waveform period. The instantaneous frequency is $f(t) = \frac{1}{2\pi}\frac{d}{dt}\left(\pi\alpha t^2\right) = \alpha t$, then we can verify that the waveform bandwidth is $B = \alpha T$. Now, we can build a set of L orthogonal chirp waveforms as [15]

$$\Phi_i(t) = \Pi_T(t) \times e^{j\pi\frac{L}{T^2}\left(t-i\frac{T}{L}\right)^2}, 0 \leq t < T, \tag{5}$$

with $\alpha = \frac{L}{T^2}$ and $i = 0, \ldots, L-1$. The maximum number of waveforms per satellite is $L = B \cdot T$. Moreover, one can show that the chirp waveforms $\Phi_i(t)$ are mutually orthogonal,

$$\begin{aligned}
&\int_0^T \Phi_m(t)\Phi_n^*(t)dt = \int_0^T e^{j\pi\frac{L}{T^2}\left(t-m\frac{T}{L}\right)^2} e^{-j\pi\frac{L}{T^2}\left(t-n\frac{T}{L}\right)^2} dt = \\
&Te^{-j\frac{\pi}{L}\left(m^2-n^2\right)} e^{-j\pi(n-m)} sinc\left(\pi(n-m)\right) = T\delta(n-m).
\end{aligned} \tag{6}$$

with $n = 0, \ldots, L-1$ and $m = 0, \ldots, L-1$. The set of chirps allows to generate a family of waveforms which can be used to demodulate non-binary symbols using a bank of matched filters. However, to correctly demodulate non-binary symbols, it is required to be synchronized with the corresponding satellite. This requires good auto-correlation and cross-correlation properties. The absolute value of the LFM autocorrelation function (ACF) is

$$\left|R_{\Phi_i}(\tau)\right| = T\left|1-\frac{\tau}{T}\right| \cdot \left|sinc\left(\pi B\tau - \frac{\pi B\tau^2}{T}\right)\right|, \tag{7}$$

where a higher bandwidth B allows to better estimate the delay parameter. A closed-form expression of the cross-correlation function (CCF) between CSS waveforms is not easy to obtain. However, we provide a numerical example in Fig. 1 to shown that the chirp family does not provide good CCF properties (i.e., low cross-correlation values). In this case, we consider a subset of 4 chirp waveforms ($i = 1, 11, 21, 31$) with $B = 1.5$ MHz and $T = 1$ms. The CCF is computed with respect to (w.r.t.) the $i = 1$ waveform. The high cross-correlation values shown in Fig. 1 generate a delay estimation ambiguity under noisy scenarios, which may induce a significant performance degradation. Moreover, such multiple peaks in the delay domain make difficult to acquire the correct satellite.

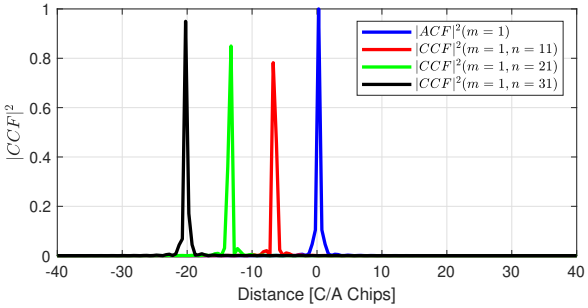

Fig. 1. Normalized $|CCF|^2$ of a subset of chirp waveforms ($i = 1, 11, 21, 31$) with $B = 1.5$ MHz and $T = 1$ms.

In order to improve the cross-correlation values of standalone chirp waveforms, we propose to change $\Pi_T(t)$ in (4) by a BCS sequence which contains a PRN sequence of period T, $\Pi_{PRN}(t)$. The non-binary PRN-Chirp modulation family is

$$\Phi_{i,p}(t) = \Pi_{PRN,p}(t) \times e^{j\pi\frac{L}{T^2}\left(t-i\frac{T}{L}\right)^2}, 0 \leq t < T, \tag{8}$$

where each satellite transmits a different PRN sequence p, from a PRN family such as Gold or Kasami [16]. Note that $\Phi_{i,p}(t)$ represent the set of symbols transmitted by the satellite (the baseband signal vector in (3) is now $\mathbf{s} = \left(\ldots, \Phi_{i,p}\left(kT_s\right), \ldots\right)^\top$). This set of waveforms has good cross-correlation properties since the CCF contains the cross-correlation function of the PRN sequence (refer to Fig. 2, where the maximum of the $|ACF|^2(m=1)$ is equal to 1). As in the standalone chirp case (6), it is easy to see that these PRN-Chirp waveforms remain mutually orthogonal,

$$\begin{aligned}
&\int_0^T \Pi_{PRN,p}(t)e^{j\pi\frac{L}{T^2}\left(t-m\frac{T}{L}\right)^2}\Pi_{PRN,p}^*(t)e^{-j\pi\frac{L}{T^2}\left(t-n\frac{T}{L}\right)^2}dt \\
&= \int_0^T |\Pi_{PRN,p}(t)|^2 e^{j\pi\frac{L}{T^2}\left(t-m\frac{T}{L}\right)^2} e^{-j\pi\frac{L}{T^2}\left(t-n\frac{T}{L}\right)^2} dt \\
&= Te^{-j\frac{\pi}{L}\left(m^2-n^2\right)} e^{-j\pi(n-m)} sinc\left(\pi(n-m)\right) = T\delta(n-m),
\end{aligned} \tag{9}$$

since $|\Pi_{PRN,p}(t)|^2$ is a constant unitary function, which allows non-binary demodulation once synchronized.

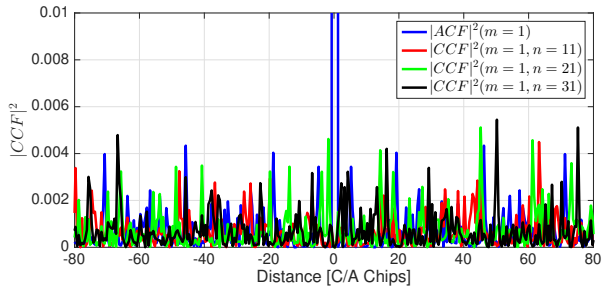

Fig. 2. Normalized $|CCF|^2$ of a subset of PRN-Chirp waveforms ($i = 1, 11, 21, 31$) with chirp waveforms with $B = 0.5$ MHz and $T = 1$ms and BPSK-modulated Gold PRN sequence with 1023 chips and duration $T = 1$ms.

A. How to Select the Non-Binary PRN-Chirp Family Set

A question of practical interest is how to select a suitable non-binary PRN-Chirp family set. Note that each waveform differs from any other waveform by a simple frequency shift equal to $\frac{(n-m)}{T}$. Then, in order to avoid a possible symbol ambiguity we must require $\frac{(n-m)}{T}$ to be larger than the Doppler effect or any frequency shift that the baseband signal might suffer (e.g., due to an unstable intermediate frequency local oscillator). Intuitively, the good option is to select the symbols as far apart as possible in the frequency domain, and the maximum number of symbols is limited by the expected Doppler. This can also play an important role in data mapping and navigation message structure design in order to improve the data demodulation conditions of the GNSS receiver.

B. Receiver Structure

A simple receiver structure that allows both to perform satellite synchronization, as well as to demodulate the non-binary symbols is constructed as a bank of parallel filters matched to each possible waveform $\{i, p\}$, where i represents the transmitted symbol and p the PRN sequence,

$$\mathbf{y}_{\{i,p,b\}} = \text{ifft}\left(\text{fft}\left(\mathbf{x}\right) \circ \text{fft}\left(\mathbf{s}_{\{i,p,b\}}\right)\right) \tag{10}$$

where $\mathbf{s}_{\{i,p,b\}} = (\ldots, \Phi_{i,p}(kT_s)e^{-j2\pi f_c(b(kT_s))}, \ldots)^\top$ for a given Doppler parameter b, $\circ$ represents the element-wise product, fft and ifft represent the direct and inverse fast Fourier transforms, and $\mathbf{y}_{\{i,p,b\}}$ is a vector which contains the samples of the matched filter output for each possible delay shift and a particular Doppler parameter b. The matrix $\mathbf{Y}_{\{i,p\}}$ (i.e., delay/Doppler map for a given PRN-Chirp waveform $\{i, p\}$) with column vectors $\mathbf{y}_{\{i,p,b\}}$ contains all the information of interest: i) if we compute $|\mathbf{Y}_{\{\mathbf{i},\mathbf{p}\}}|^2$ for a given PRN sequence p and the set of symbols i, it is possible to construct an acquisition stage to be used for satellite detection; ii) if a given satellite is detected, the maximum output value from the subset of matched filters with equal sequence p, $|\mathbf{Y}_{\{\mathbf{i}\}}|^2$, provides a decision about the received symbol; and iii) for a given detected satellite, the arguments that maximize the delay-Doppler map function provide the delay/Doppler maximum likelihood estimates (MLE) $\hat{\boldsymbol{\eta}} = \{\hat{\tau}, \hat{b}\}$.

Unlike for current GNSS modulations, the phase knowledge is not required to demodulate the data since the metric used to retrieve it is $|\mathbf{Y}_{\{\mathbf{i}\}}|^2$. However, if a phase estimate is available (e.g., at the tracking stage) the data demodulation performance can be improved (refer to Sec. V). It is worth pointing out that on Earth the maximum Doppler and Doppler rate are around 5 KHz and 1 Hz/s, then the Gaussian channel applies.

IV. CRB, MLE and Symbol Error Rate

The ultimate achievable performance on the mean square error (MSE) sense is brought by the corresponding Cramér-Rao lower bound (CRB), which gives an accurate MSE estimation of the MLE in the asymptotic region. Considering (3), the MLE of $\boldsymbol{\eta}$ is (known signal replica at the receiver)

$$\widehat{\boldsymbol{\eta}} = \arg\max_{\boldsymbol{\eta}} \left\{ \frac{\left|\mathbf{a}(\boldsymbol{\eta})^H \mathbf{x}\right|^2}{\mathbf{a}(\boldsymbol{\eta})^H \mathbf{a}(\boldsymbol{\eta})} \right\}, \tag{11}$$

and the maximum SNR at the output of the MLE matched filter is $\text{SNR}_{\text{out}} = \frac{|\alpha|^2 \mathbb{E}}{(\sigma_{\mathbf{n}}^2/F_s)}$, with $\mathbb{E} = \int_{-\infty}^{+\infty} |s(t)|^2 dt$ the signal energy. It is worth pointing out that the phase MLE is given by the argument of the cross-ambiguity function evaluated at $\widehat{\boldsymbol{\eta}}$, $\widehat{\varphi}(\widehat{\boldsymbol{\eta}}) = \arg\left\{\left(\mathbf{a}^H(\widehat{\boldsymbol{\eta}})\,\mathbf{a}(\widehat{\boldsymbol{\eta}})\right)^{-1}\mathbf{a}^H(\widehat{\boldsymbol{\eta}})\,\mathbf{x}\right\}$. If we define

$$\boldsymbol{\Omega}(\boldsymbol{\eta}) = \frac{\partial \mathbf{a}(\boldsymbol{\eta})}{\partial \boldsymbol{\eta}^T}^H \boldsymbol{\Pi}^{\perp}_{\mathbf{a}(\boldsymbol{\eta})} \frac{\partial \mathbf{a}(\boldsymbol{\eta})}{\partial \boldsymbol{\eta}^T} = \left\| \frac{\partial \mathbf{a}(\boldsymbol{\eta})}{\partial \boldsymbol{\eta}^T} \right\|^2 - \frac{\left| \mathbf{a}(\boldsymbol{\eta})^H \frac{\partial \mathbf{a}(\boldsymbol{\eta})}{\partial \boldsymbol{\eta}^T} \right|^2}{\|\mathbf{a}(\boldsymbol{\eta})\|^2}, \tag{12}$$

the CRB of $\boldsymbol{\eta}$ is $\mathbf{CRB}_{\boldsymbol{\eta}} = \frac{\sigma_n^2}{2|\beta|^2}\text{Re}\{\boldsymbol{\Omega}(\boldsymbol{\eta})\}^{-1}$. The compact $\text{Re}\{\boldsymbol{\Omega}(\boldsymbol{\eta})\}$ expression is given in [12]. Even if for complex signals the delay, Doppler and phase estimation are not decoupled as in the real signal case, for GNSS signals it has been shown that the impact is negligible [17].

In order to evaluate the data demodulation performances several metrics can be used. In this contribution, since we do not consider any particular channel coding strategy , we use the symbol error rate (SER) as a meaningful metric.

V. Results and Discussion

In order to validate the new GNSS waveform, we assess both the delay estimation performance and the SER for different representative scenarios. We consider a PRN-Chirp family set constructed from a BPSK-modulated Gold PRN sequence, with 1023 chips and duration $T = 1$ ms. The chirp family is generated with $B = 0.5$ MHz and $T = 1$ ms, and we select 4 possible cases with $2^M = \{4, 8, 16, 32\}$ symbols. The symbols are selected to be as separate as possible in the frequency band in order to avoid any possible symbol ambiguity. We illustrate the PSDs for the 2 subsets $\{4, 32\}$ in Fig. 3, which are almost equal. However, those PSDs slightly occupy more spectral band w.r.t. the BPSK case (i.e., in case of selecting symbols closer in frequency, the spectral efficiency would increase).

A. Joint Synchronization and Data Demodulation

In a first scenario, we consider the most general case where the receiver has to perform both delay/Doppler synchronization and data demodulation, as detailed in Section III-B. Notice

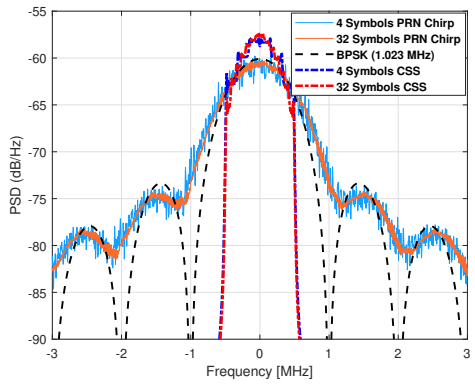

Fig. 3. PSD of non-binary PRN-Chirp modulation families with $2^M = \{4, 32\}$ symbols vs PSD of the BPSK modulation and CSS.

that this is not possible with CSK and CSS modulation, which need to be synchronized.

The delay estimation performance for the different subsets of waveforms is shown in Fig. 4, where we considered $F_s = 2.046$MHz. Notice that the MLE performance (root mean square error (RMSE) w.r.t. the SNR_{out} and obtained from 50000 Monte Carlo runs) is compared to the CRB obtained for the standalone Gold PRN sequence, as the CRBs for the different waveforms are almost equivalent to it. Notice that independently of the symbol subset the MLE converges to the corresponding CRB after a certain threshold region around 15.5 dB. Such results confirm that the delay estimation performance in the asymptotic region is independent of the cardinality of the waveform set. In addition, the threshold region is the same for the four waveform sets, being also equivalent to the standalone Gold PRN performance [12]. This validates that in terms of synchronization performance, the new PRN-Chirp waveform is equivalent to the standalone PRN counterpart, then providing the PVT estimation performance.

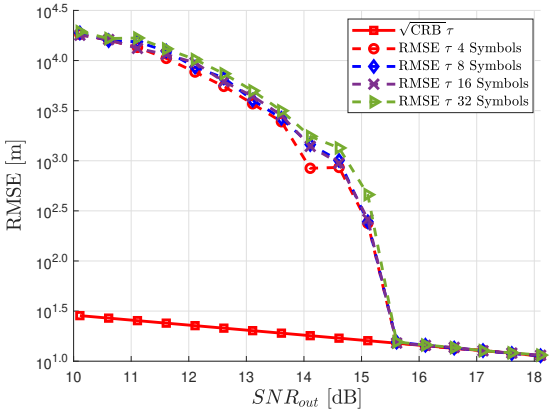

Fig. 4. Delay CRB for the GPS C/A Gold PRN sequence #1, and delay MLE for the non-binary PRN-Chirp modulation families with $2^M = \{4, 8, 16, 32\}$ symbols and $F_s = 2.046$ MHz.

Considering the same scenario, the SER results for the different sets are shown in Fig. 5, as a function of the SNR_{out}. We assume that the phase is unknown, and both delay and Doppler are being estimated through MLE, then, a non-coherent demodulation is required. For completeness we consider two cases: 1) delay and Doppler estimation, termed "Delay/Doppler Est" and shown with dashed lines, and 2) perfect Doppler removal and only the delay is estimated, termed "Delay Est" and shown with solid lines.

First, in both cases the SER is logically degraded as a function of the set cardinality, but in any case, considering the time-delay estimation threshold for an optimal receiver operation point the SER is always below 10^{-3}. In addition, we can see that considering a perfect Doppler removal the SER is slightly improved, but such marginal degradation (i.e., when estimating the Doppler) validates the good behaviour of the proposed receiver architecture. Finally, we must point out that this scheme allows to demodulate the data during the synchronization time, decreasing the time needed to demodulate the navigation message. Moreover, being able to demodulate symbols instead of bits, also allows to reduce the TTD.

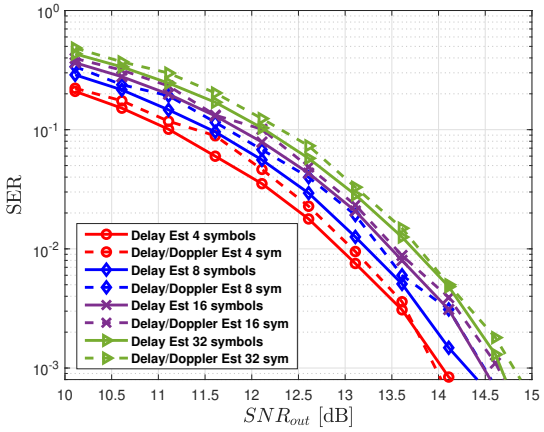

Fig. 5. SER for the non-binary PRN-Chirp modulation, with $2^M = \{4, 8, 16, 32\}$ symbols, without delay (and Doppler) synchronization.

B. Synchronized Data Demodulation Performance: PRN-Chirp vs CSK Modulations

In a second scenario, we assess the SER considering that delay and Doppler are perfectly estimated but the knowledge of the phase is still not available at the receiver, i.e., non-coherent demodulation is required. The SER for the non-binary PRN-Chirp with $2^M = \{4, 8, 16, 32\}$ symbols (solid lines) is shown in Fig. 6. First, note the SER performance improvement w.r.t. the previous scenario without perfect synchronization (refer to Fig. 5). As an example, for 4 symbols we have an improvement of 2.5 dB for a SER of 10^{-3}. Because we consider a perfect synchronization, we can compare the proposed modulation with other well-known non-binary modulations such as the CSK. Then, in Fig. 6 we also illustrate the SER (dashed lines) of the non-binary CSK modulation with $2^M = \{4, 8, 16, 32\}$ symbols and also considering the Gold PRN #1 sequence. Notice that the SER of both modulations is almost equivalent. The reason why the SER is almost the same is because even if the CSK modulation is not perfectly orthogonal, when the PRN sequences are long enough (e.g., 1023 chips), this

modulation is quasi-orthogonal. These results validate again the good performance of the proposed approach.

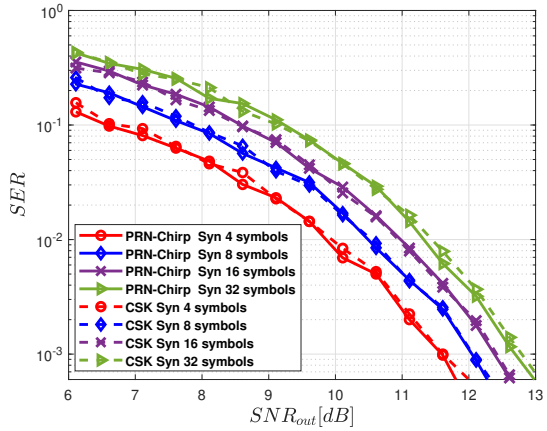

Fig. 6. SER of the non-binary PRN-Chirp and CSK modulations with $2^M = \{4, 8, 16, 32\}$ symbols. Perfect delay/Doppler synchronization is assumed, but no phase information is available.

C. Coherent Demodulation: PRN-Chirp vs CSK Modulations

In the last representative scenario we consider a perfect knowledge of the phase at the receiver (as well as perfect delay and Doppler synchronization). This implies that the phase estimation (either through a MLE or obtained from the tracking) is performed properly, which can be considered for nominal channel conditions where no multipath, shadowing or interefernece are present. Under coherent demodulation, the output of the matched filter (in contrast to the non-coherent $|\cdot|^2$) is considered to compute the SER. SER results for both PRN-Chirp (solid lines) and CSK (dashed lines) modulations, with $2^M = \{4, 8, 16, 32\}$ symbols, are shown in Fig. 7. We can notice again that i) the SER performance, as expected, is further improved w.r.t. the previous non-coherent demodulation case in Fig. 6, and ii) the SER for both modulations is almost equivalent, because the CSK modulation is quasi-orthogonal when the PRN sequences are long enough.

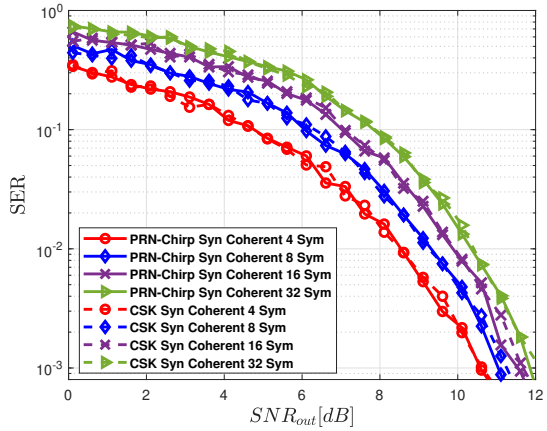

Fig. 7. SER of the non-binary PRN-Chirp and CSK modulations with $2^M = \{4, 8, 16, 32\}$ symbols. Perfect synchronization and phase knowledge.

VI. Conclusion

In this contribution, we proposed a new non-binary modulation which allows to perform both GNSS acquisition and tracking (i.e., delay and Doppler synchronization), as well as to demodulate non-binary symbols without the need of a pilot signal. Thanks to this new non-binary modulation, the receiver is potentially able to provide a faster first PVT solution fix, by decreasing the TTD. In order to design the set of waveforms we propose to exploit the product of two well-known families of modulations. The first family is constructed from PRN sequences, which have good auto-correlation and cross-correlation properties. The second modulation set is a CSS family which allows to demodulate non-binary symbols even if the phase knowledge is unknown. In order to demodulation the data, a bank of non-coherent matched filters is proposed. The simulation results showed the good performance of the proposed new waveform, both in terms of synchronization and data demodulation capabilities. The joint synchronization and data demodulation allows to decrease the TTD, while properly dealing with the baseband signal processing receiver functionalities.

References

[1] B. Schotsch *et al.*, "Joint Time-to-CED Reduction and Improvement of CED Robustness in the Galileo I/NAV Message." Proc. of the ION GNSS+, 2017.
[2] L. Ortega *et al.*, "New Solutions to Reduce the Time-To-CED and to Improve the CED Robustness of the Galileo I/NAV Message." Proc. of the IEEE/ION PLANS, 2018.
[3] P. J. G. Teunissen and O. Montenbruck, Eds., *Handbook of Global Navigation Satellite Systems*. Switzerland: Springer, 2017.
[4] M. Anghileri *et al.*, "Reduced Navigation Data for a Fast First Fix." Proc. of the ESA Navitec, 2012.
[5] M. Paonni and M. Bavaro, "On the Design of a GNSS Acquisition Aiding Signal." Proc. of the ION GNSS+,, 2013.
[6] L. Ortega *et al.*, "Optimizing the Co-Design of Message Structure and Channel Coding to Reduce the TTD for a Galileo 2nd Generation Signal," *Navigation*, 2020.
[7] M. Roudier, "Analysis and Improvement of GNSS Navigation Message Demodulation Performance in Urban Environments," Ph.D. dissertation, INP Toulouse, Jan 2015.
[8] L. Ortega, J. Vilà-Valls, C. Poulliat, and P. Closas, "GNSS Data Demodulation over Fading Environments: Antipodal and M-ary CSK Modulations," *IET Radar, Sonar & Navigation*, vol. 15, no. 2, Feb. 2021.
[9] E. Sénant *et al.*, "Tentative New Signals and Services in Upper L1 and S Bands for Galileo Evolutions." Proc. of the ION GNSS+, 2018.
[10] J. Rodriguez, "On Generalized Signal Waveforms for Satellite Navigation," Ph.D. dissertation, Universitätsbibliothek der Universität der Bundeswehr München, 2008.
[11] A. Roy, H. B. Nemade, and R. Bhattacharjee, "Performance of Multiuser Communication System Using Phase Coded Linear Chirp Modulation," in *23rd National Conference on Communications (NCC)*, 2017.
[12] D. Medina, L. Ortega, J. Vilà-Valls, P. Closas, F. Vincent, and E. Chaumette, "Compact CRB for Delay, Doppler and Phase Estimation - Application to GNSS SPP & RTK Performance Characterization," *IET Radar, Sonar & Navigation*, vol. 14, no. 10, pp. 1537–1549, Sep. 2020.
[13] A. Dogandzic and A. Nehorai, "Cramér-Rao Bounds for Estimating Range, Velocity, and Direction with an Active Array," *IEEE Trans. Signal Process.*, vol. 49, no. 6, pp. 1122–1137, June 2001.
[14] M. I. Skolnik, *Radar Handbook*, 3rd ed. New York, USA: McGraw-Hill, 1990.
[15] X. Ouyang and J. Zhao, "Orthogonal Chirp Division Multiplexing," *IEEE Trans. on Communications*, vol. 64, no. 9, pp. 3946–3957, 2016.
[16] J. K. Holmes, *Spread spectrum systems for GNSS and wireless communications*. Artech House Norwood, MA, 2007.
[17] P. Das, L. Ortega, J. Vilà-Valls, F. Vincent, E. Chaumette, and L. Davain, "Performance limits of gnss code-based precise positioning: Gps, galileo & meta-signals."